



## Regularized inversion for subsalt imaging: real data example

Marie L. Clapp and Robert G. Clapp<sup>1</sup>

### ABSTRACT

Imaging the subsurface where seismic illumination is poor is a difficult exercise. Conventional imaging techniques such as migration are insufficient. Better results can be obtained from regularized least-squares inversion methods that use migration operators in a conjugate-gradient minimization. We demonstrate this regularized inversion using downward continuation migration and regularization along offset ray parameters (reflection angles) on a real 2-D seismic line. The result is cleaner than the migration result and has filled in some amplitude information where poor illumination caused gaps. We discuss a regularized inversion that uses common azimuth migration and the same type of regularization to image a real 3-D subsurface around a salt body.

### INTRODUCTION

Properly imaging the subsurface in areas that are structurally complex is a daunting task. The migration algorithms typically used for imaging are unable to provide satisfactory images where shadow zones are common, particularly around salt bodies (Muerdter et al., 1996; Prucha et al., 1998). Since salt can make a good hydrocarbon trap, these areas are where we would really like to obtain good images.

There have been many improved migration algorithms that ameliorate the effects of the complex subsurface. Several authors have demonstrated that wave equation migration methods can provide better images than Kirchhoff migration methods (Geoltrain and Brac, 1993; O'Brien and Etgen, 1998). Additionally, some artifacts commonly seen in complex areas are caused by seismic energy that arrives at the receivers at the same time, but follow different paths through and reflect at different points in the subsurface (ten Kroode et al., 1994). These artifacts can be reduced by creating images with angle-domain common image gathers (ADCIGs). Methods that produce ADCIGs through Kirchhoff techniques (Xu et al., 2001) may partially reduce artifacts caused by multipathing, but still have difficulties (Stolk and Symes, 2002). Wave equation methods to create ADCIGs (Prucha et al., 1999; Mosher and Foster, 2000) handle multipathing better (Stolk and De Hoop, 2001; Stolk and Symes, 2004). However, regardless of how a migration algorithm is formulated, migration is generally insufficient to image poorly illuminated areas (Prucha et al., 2001).

To improve our seismic imaging in areas of poor illumination, we can use migration as

---

<sup>1</sup>email: marie @ sep.Stanford.edu, bob @ sep.Stanford.edu

an imaging operator in a least-squares inversion scheme (Nemeth et al., 1999; Duquet and Marfurt, 1999; Ronen and Liner, 2000; Prucha and Biondi, 2002b; Kuehl and Sacchi, 2001). In areas with poor illumination, the inversion problem is ill-conditioned; therefore, it is wise to regularize the inversion (Tikhonov and Arsenin, 1977). The regularization operator can be designed to exploit knowledge we have about the expected amplitude behavior and dip orientation of events in the image (Prucha and Biondi, 2002a).

In this paper, we will begin by reviewing a scheme for iterative regularized inversion. We will implement an inversion scheme that regularizes amplitudes along offset ray parameters (reflection angles) on a real 2-D seismic line from the Gulf of Mexico. We will also discuss how our regularized inversion scheme that can be applied to the real 3-D dataset from which we extracted the 2-D line.

## REVIEW OF REGULARIZED INVERSION

The vast size of the seismic imaging problems makes performing a direct inversion impossible with today's computer power, even if we are only dealing with a 2-D seismic line. Fortunately, we can closely approximate a direct inverse with iterative techniques. In particular, we can approximate a least-squares inversion with the conjugate-gradient minimization of this objective function:

$$Q(\mathbf{m}) = \|\mathbf{Lm} - \mathbf{d}\|^2 \quad (1)$$

where  $\mathbf{L}$  is a linear modeling operator,  $\mathbf{d}$  is the data, and  $\mathbf{m}$  is the model. This minimization can be expressed more concisely as a fitting goal:

$$\mathbf{0} \approx \mathbf{Lm} - \mathbf{d}. \quad (2)$$

However, for the seismic imaging problem, this inversion can have a large null space, due in part to poor illumination. Any noise that exists within that null space can grow with each iteration until the problem becomes unstable. Fortunately, we can stabilize this problem with regularization (Tikhonov and Arsenin, 1977). The regularization adds a second fitting goal that we are minimizing at the same time:

$$\begin{aligned} \mathbf{0} &\approx \mathbf{Lm} - \mathbf{d} \\ \mathbf{0} &\approx \epsilon \mathbf{Am}. \end{aligned} \quad (3)$$

The first expression is the "data fitting goal," meaning that it is responsible for making a model that is consistent with the data. The second expression is the "model styling goal," meaning that it allows us to impose some idea of what the model should look like using the regularization operator  $\mathbf{A}$ . The strength of the regularization is controlled by the regularization parameter  $\epsilon$ .

Unfortunately, the inversion process described by fitting goals (3) can take many iterations to produce a satisfactory result. We can reduce the necessary number of iterations by making

the problem a preconditioned one. We use the preconditioning transformation  $\mathbf{m} = \mathbf{A}^{-1}\mathbf{p}$  (Fomel et al., 1997; Fomel and Claerbout, 2003) to give us these fitting goals:

$$\begin{aligned}\mathbf{0} &\approx \mathbf{L}\mathbf{A}^{-1}\mathbf{p} - \mathbf{d} \\ \mathbf{0} &\approx \epsilon\mathbf{p}.\end{aligned}\tag{4}$$

$\mathbf{A}^{-1}$  is obtained by mapping the multi-dimensional regularization operator  $\mathbf{A}$  to helical space and applying polynomial division (Claerbout, 1998). This process is called Regularized Inversion with model Preconditioning (RIP).

### The migration operator

The migration operator and its adjoint ( $\mathbf{L}$ ) that are used in this inversion scheme are linear operators. For the 2-D case, we choose to use the downward continuation migration operator introduced by Prucha et al. (1999). This 2-D downward continuation migration operator takes an input of seismic data with the dimensions of common midpoint (CMPX), offset ( $h_x$ ), and frequency ( $\omega$ ). Its output is a model (image) with the dimensions of depth ( $z$ ), common reflection point (CRPX), and offset ray parameter ( $p_{hx}$ ), which is related to the reflection angle for a given subsurface point. This downward continuation migration operator can be formulated as a 3-D process by adding the crossline common midpoint (CMPY) and crossline offset ( $h_y$ ) to the input, but that would be a very computationally expensive process. Fortunately, to reduce costs in 3-D, we could also use a Common Azimuth Migration (CAM) operator (Biondi and Palacharla, 1996). For this, we add the CMPY dimension, but not the crossline offset.

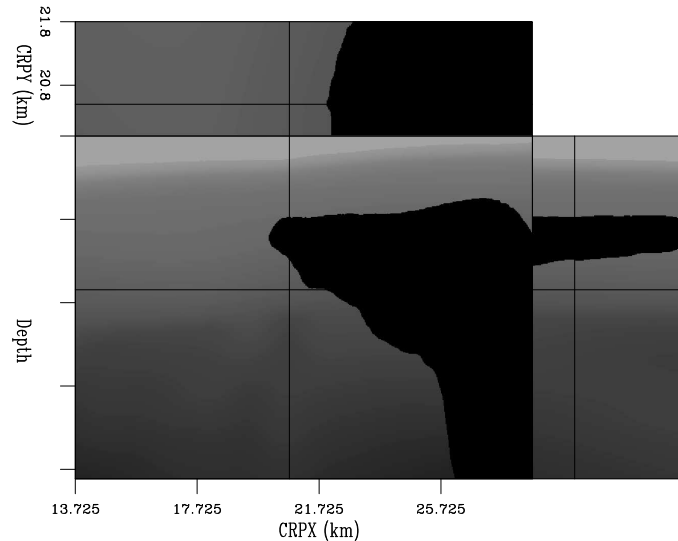
### The regularization operator

The regularization operator ( $\mathbf{A}$ ) should be designed based on the expected model covariance (Tarantola, 1986). Since we are particularly concerned with the effects of poor illumination, we need to design  $\mathbf{A}$  to compensate for these effects. In this case, since our downward continuation operator or CAM operator will create a model that is a cube of depth, CRPX, CRPY (for the CAM operator), and  $p_{hx}$ , we can expect illumination problems to appear as gaps in events in the CRP plane(s) and along the  $p_{hx}$  axis. Prucha et al. (2001) demonstrated the use of steering filters (Clapp et al., 1997) as a regularization operator to compensate for sudden changes in amplitude along events with an expected dip. Accomplishing this in the CRP planes requires some interpretation of the result of migration, but along the  $p_{hx}$  we expect the events to be flat and horizontal as long as the correct velocities have been used for imaging. In this paper, to keep  $\mathbf{A}$  simple, we will just be applying the steering filters horizontally along the  $p_{hx}$  axis. This regularization scheme will minimize changes in amplitude along the  $p_{hx}$  axis, penalizing large amplitude changes the most.

## RESULTS

To demonstrate our 2-D Regularized Inversion with model Preconditioning (RIP), we choose to extract a 2-D line from a real 3-D Gulf of Mexico dataset provided to us by BP and Exxon-Mobil. A portion of the 3-D velocity model for this dataset can be seen in Figure 1. The velocity model is believed to be accurate, which is important given our choice of regularization operator (Clapp, 2003).

Figure 1: Subset of the BP Gulf of Mexico velocity model. `marie2-bpvel` [CR]



We first performed downward continuation migration on this 2-D line. The migration results can be seen in Figures 2 and 4. In these figures, the left part shows a common offset ray parameter section, taken from  $p_{hx} = .153$  and  $p_{hx} = .317$  respectively. The right part shows a common image gather taken from  $CRPX = 20.5$  and  $CRPX = 22.225$  respectively.

In Figure 2, note the clear shadow zones visible in the common offset ray parameter section. The poor illumination that causes these shadow zones is manifested in the common image gather as gaps in the events. These gaps are what we hope to fill with our regularization operator.

Figure 3 is the result of 10 iterations of RIP. The common  $p_{hx}$  section and common image gather correspond to those of the migration result in Figure 2. The inversion process has cleaned up many of the artifacts seen in the migration result. More importantly, the common image gathers show that we are filling the gaps in the events. Our regularization operator is successfully compensating for the illumination problems.

The common  $p_{hx}$  section shown in the migration result in Figure 4 and the RIP result in Figure 5 is interesting. At the  $CRPX$  location from which we have extracted the common image gather ( $CRPX = 22.225$ ), we note that the result after 10 iterations of RIP (Figure 5 is beginning to show real events beneath the salt that are not visible in the migration result (Figure 4). The common image gather shows that we have extended the events in  $p_{hx}$ , essentially allowing the inversion image to “recapture” energy that left the survey area. Additionally, as we saw in Figure 3, the inversion result is cleaner than the migration result.

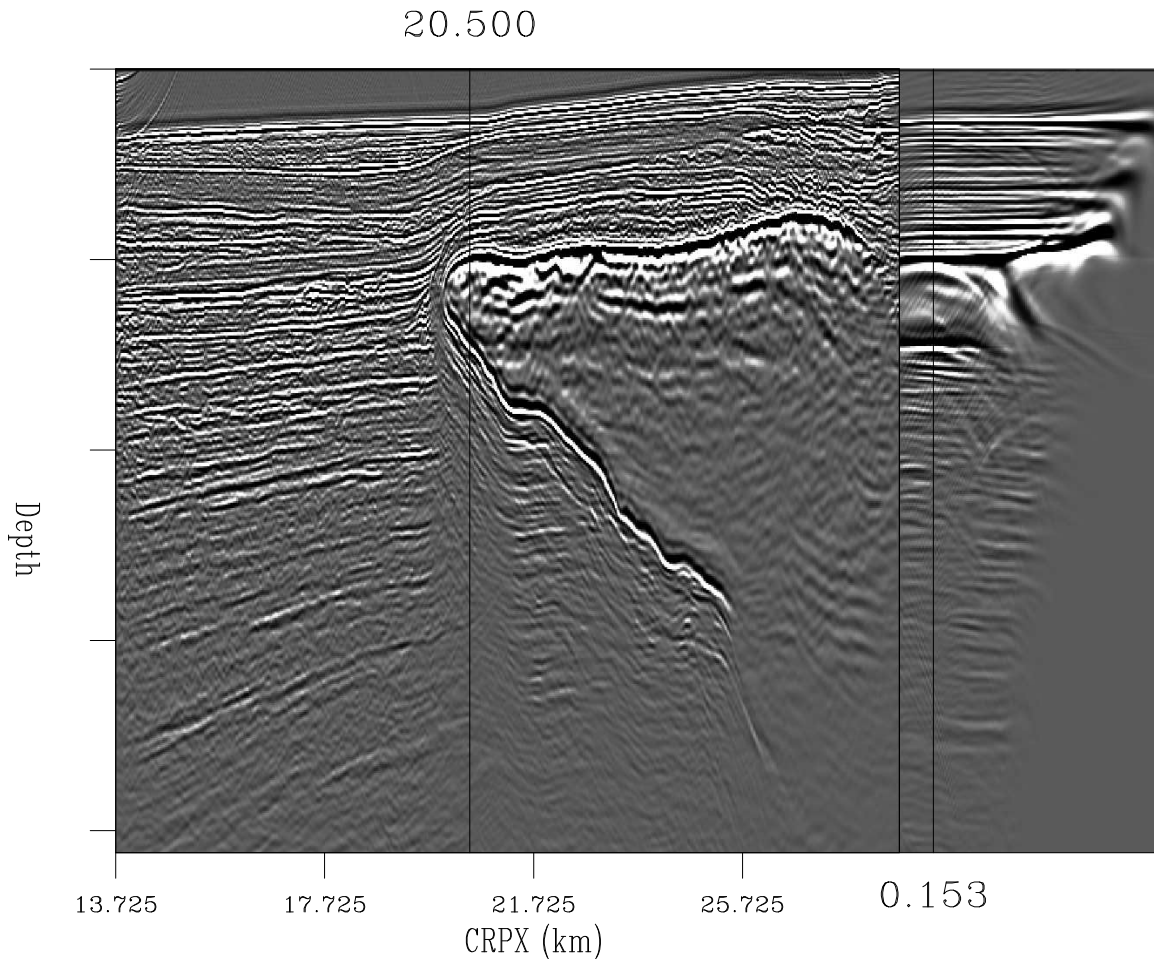


Figure 2: Result of downward continuation migration of 2-D line. Left part is a common offset ray parameter section, right part is a common image gather taken from  $CRPX = 20.5$ . `marie2-bpcube.mig2d` [CR]

It is also interesting to stack the migration and RIP results for comparison. Figure 6 shows the stacked migration result and Figure 7 shows the stacked RIP result after 10 iterations. Each of these figures has been zoomed in to concentrate on the poorly illuminated areas under the salt. The RIP stack is slightly higher in frequency content, due to artifacts in the migration result that stack into lower frequencies. More importantly, the RIP stack has improved the imaging of events within the shadow zones. The events extend farther into the poorly illuminated areas, are more continuous, and have more consistent amplitudes.

## CONCLUSIONS

The Regularized Inversion with model Preconditioning (RIP) process that we have previously used only on synthetic data has proven to be effective on real data as well. The regularization scheme used for RIP in this paper helps to compensate for poor illumination by penalizing

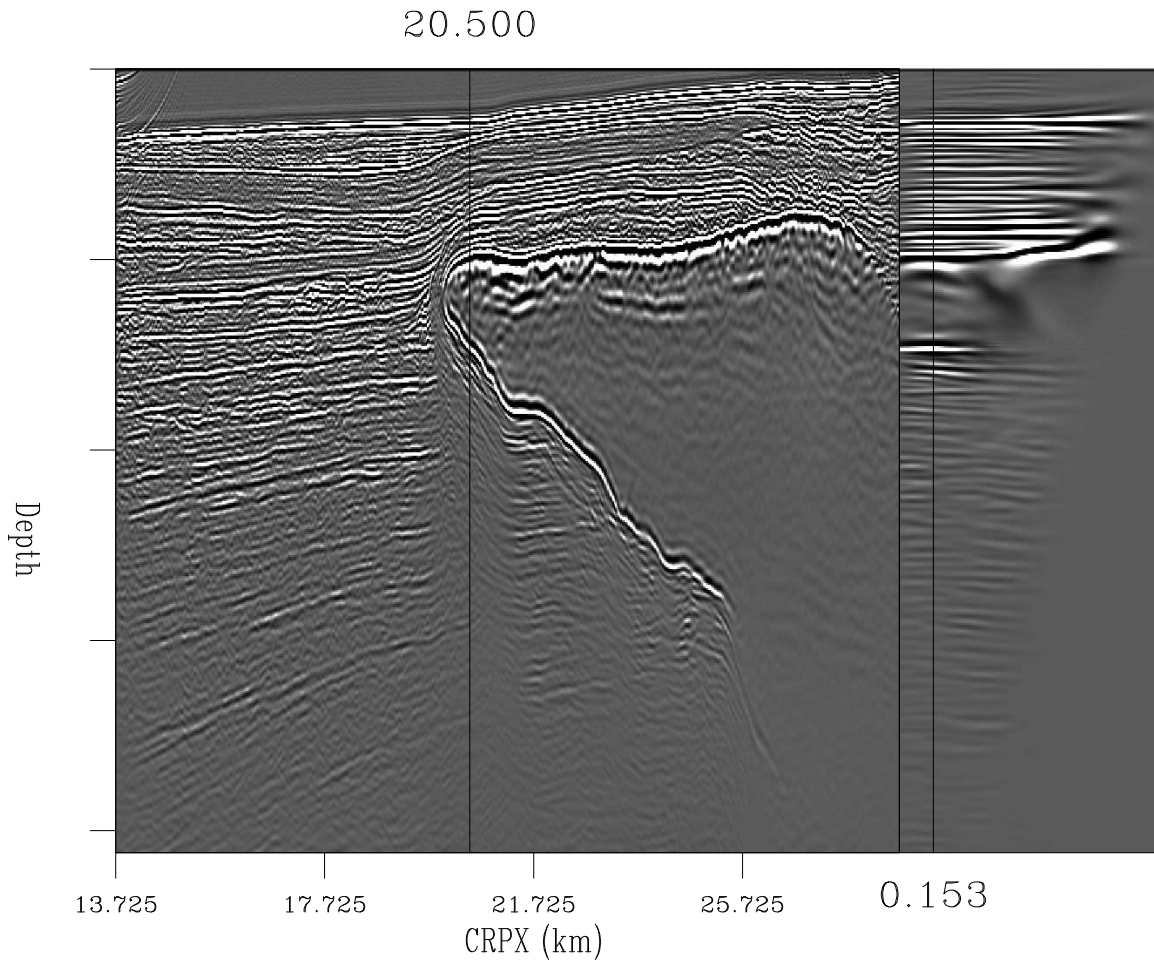


Figure 3: Result of 10 iterations of RIP. Left part is a common offset ray parameter section, right part is a common image gather taken from  $CRPX = 20.5$ . `marie2-bpcube.1dprec.10it [CR]`

large amplitude changes along the offset ray parameter axis. It also helps to clean up artifacts that plague migration results.

### FUTURE WORK

As discussed in this paper, we wish to extend RIP to work on 3-D data. We plan to do so by switching from our downward continuation migration to a Common Azimuth Migration (CAM). The regularization operator will still act along the inline offset ray parameter axis.

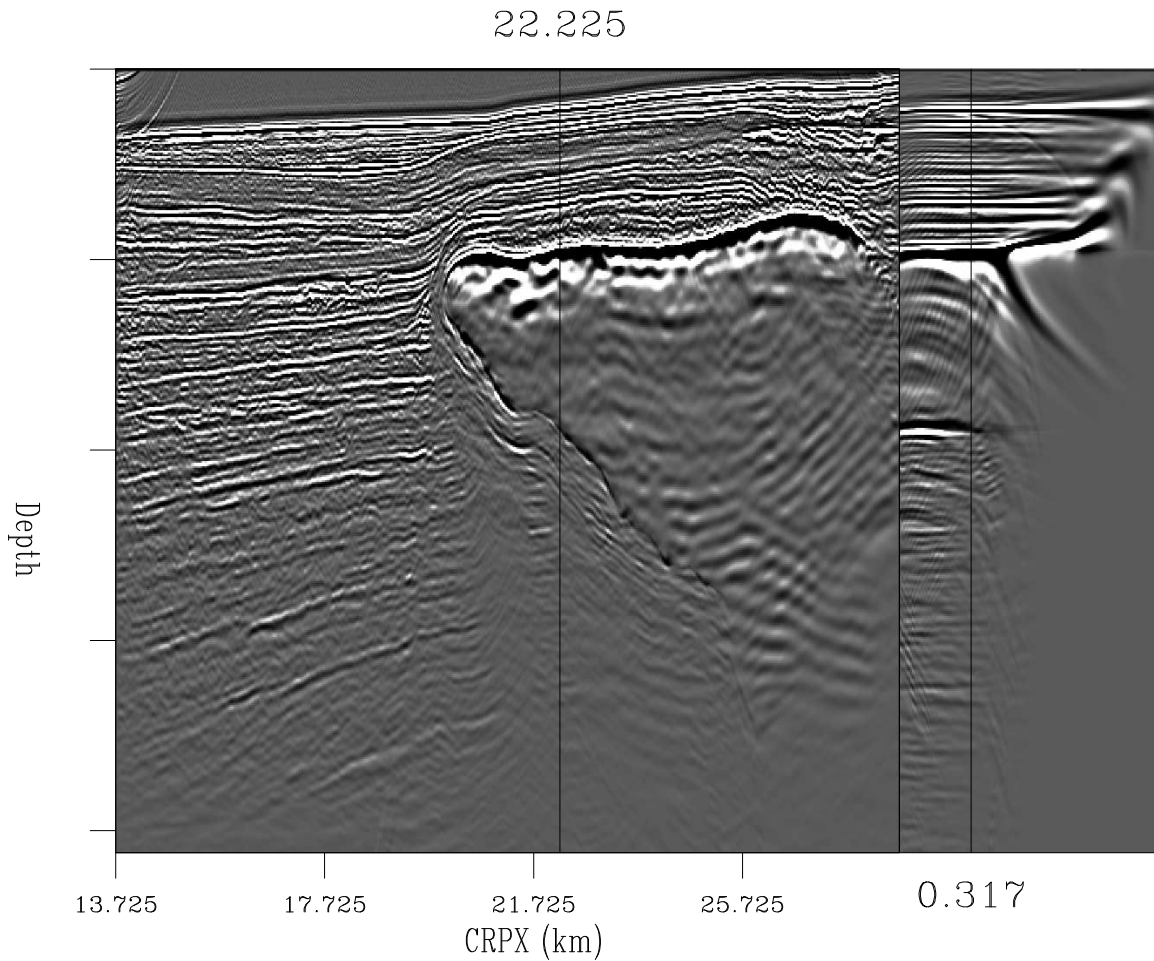


Figure 4: Result of downward continuation migration of 2-D line. Left part is a common offset ray parameter section, right part is a common image gather taken from  $CRPX = 22.225$ . `marie2-bpcubes.mig2d` [CR]

### ACKNOWLEDGMENTS

We would like to thank BP and ExxonMobil for providing SEP with the 3-D GoM dataset used in this paper.

### REFERENCES

- Biondi, B., and Palacharla, G., 1996, 3-d prestack migration of common-azimuth data: 3-d prestack migration of common-azimuth data:, Soc. of Expl. Geophys., Geophysics, 1822–1832.
- Claerbout, J., 1998, Multidimensional recursive filters via a helix: Geophysics, **63**, no. 05, 1532–1541.



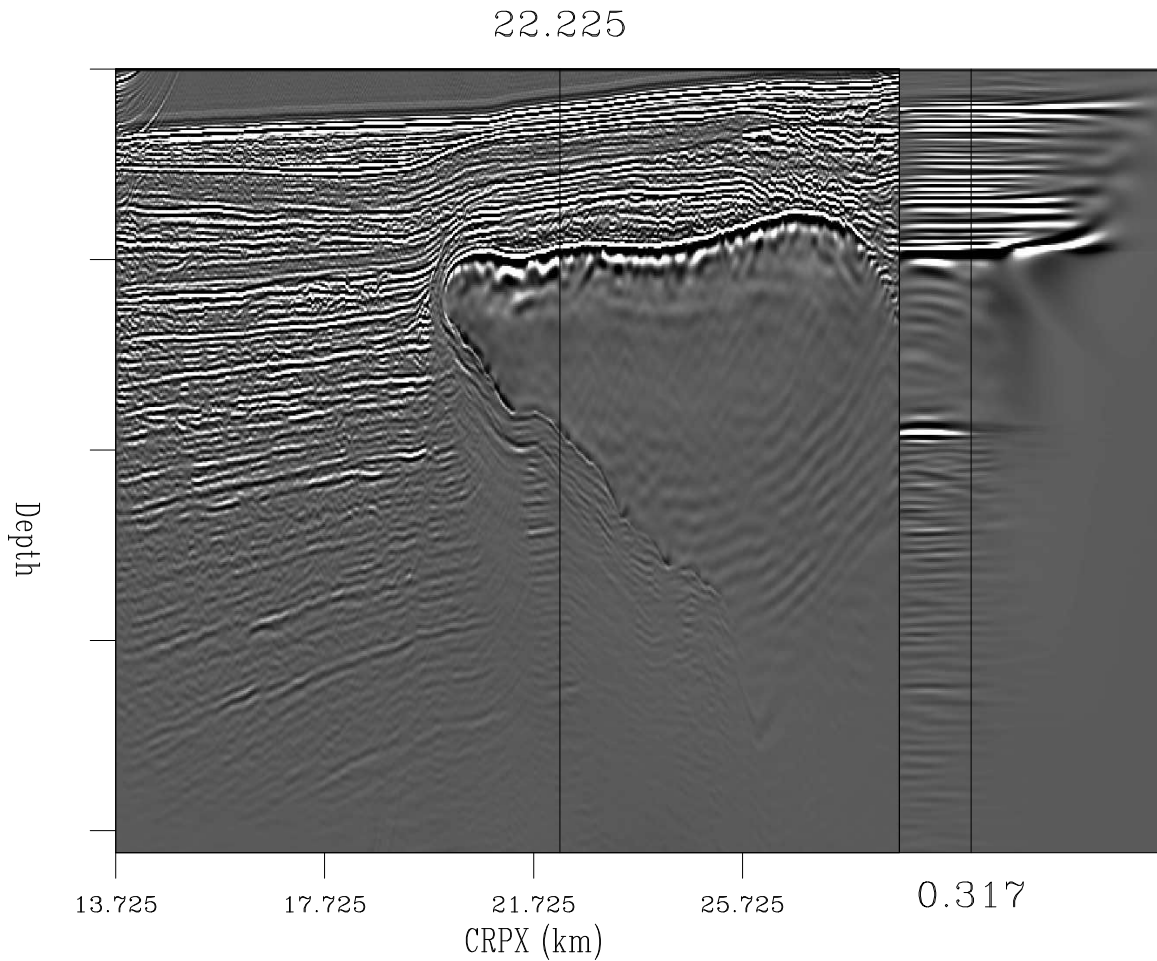


Figure 5: Result of 10 iterations of RIP. Left part is a common offset ray parameter section, right part is a common image gather taken from  $CRPX = 22.225$ .  
marie2-bpcubes.1dprec.10it [CR]

Clapp, R. G., Fomel, S., and Claerbout, J., 1997, Solution steering with space-variant filters: SEP-95, 27–42.

Clapp, M. L., 2003, Velocity sensitivity of subsalt imaging through regularized inversion: SEP-114, 57–66.

Duquet, B., and Marfurt, K. J., 1999, Filtering coherent noise during prestack depth migration: Geophysics, **64**, no. 4, 1054–1066.

Fomel, S., and Claerbout, J., 2003, Multidimensional recursive filter preconditioning in geophysical estimation problems: Geophysics, **68**, no. 2, 577–588.

Fomel, S., Clapp, R., and Claerbout, J., 1997, Missing data interpolation by recursive filter preconditioning: SEP-95, 15–25.

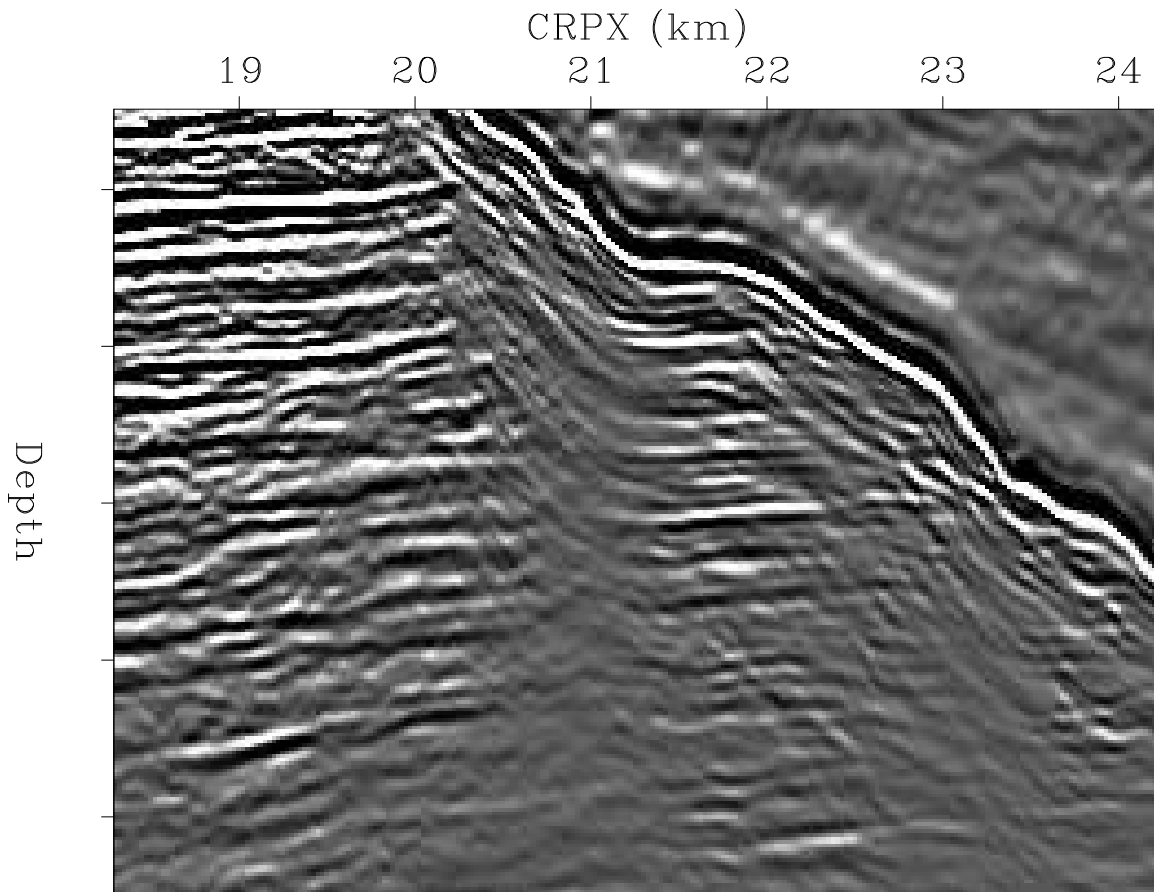


Figure 6: Stack of the downward continuation migration result, zoomed in under the salt body.  
`marie2-bpzstacks.mig2d` [CR]

Geoltrain, S., and Brac, J., 1993, Can we image complex structures with first-arrival travel-time?: *Geophysics*, **58**, no. 04, 564–575.

Kuehl, H., and Sacchi, M., 2001, Generalized least-squares dsr migration using a common angle imaging condition: 71st Ann. Internat. Meeting, Soc. Expl. Geophysics, Expanded Abstracts, 1025–1028.

Mosher, C., and Foster, D., 2000, Common angle imaging conditions for prestack depth migration:., *in* 70th Ann. Internat. Mtg Soc. of Expl. Geophys., 830–833.

Muerdter, D. R., Lindsay, R. O., and Ratcliff, D. W., 1996, Imaging under the edges of salt sheets: a raytracing study: Soc. Expl. Geophys., 66th Annual Internat. Mtg., Soc. Expl. Geophys., Expanded Abstracts, 578–580.

Nemeth, T., Wu, C., and Schuster, G. T., 1999, Least-squares migration of incomplete reflection data: *Geophysics*, **64**, no. 1, 208–221.

O'Brien, M. J., and Etgen, J. T., 1998, Wavefield imaging of complex structures with sparse

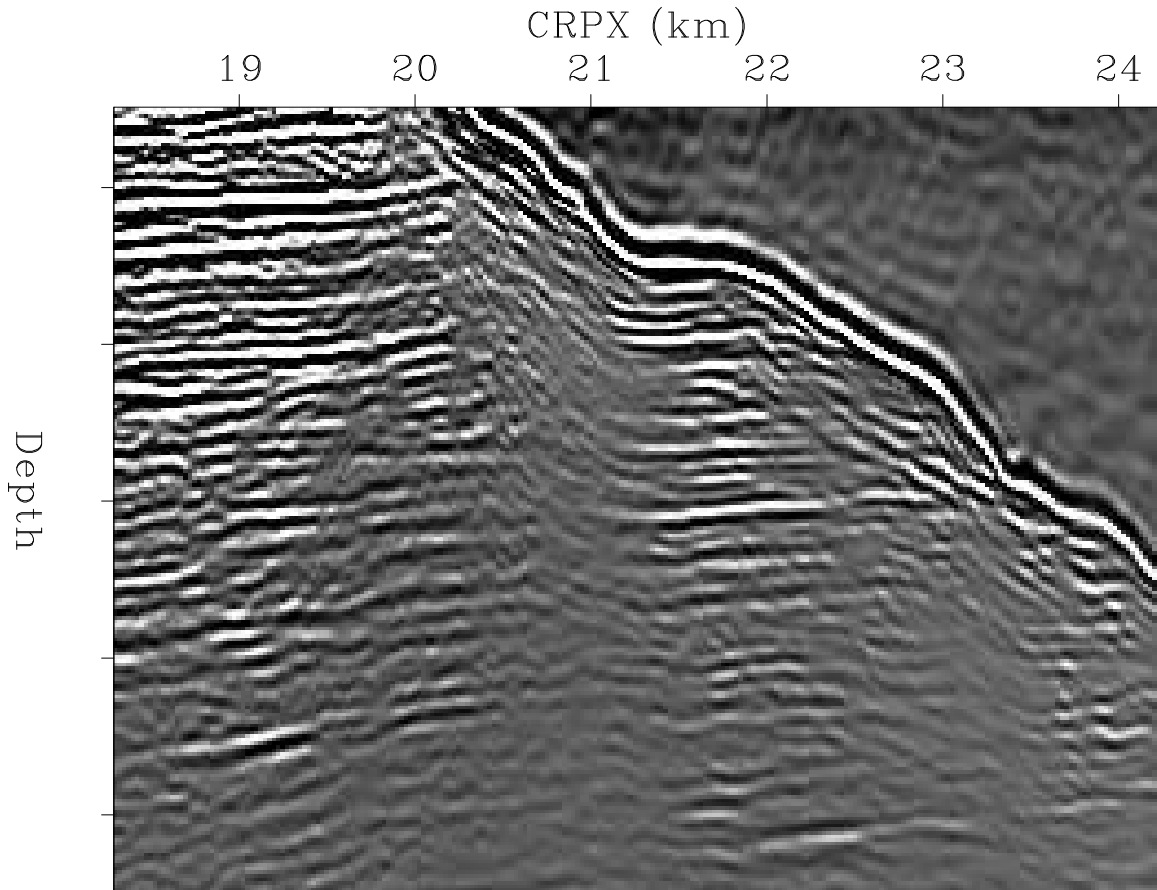


Figure 7: Stack of the RIP result after 10 iterations, zoomed in under the salt body.  
`marie2-bpzstacks.1dprec.10it` [CR]

point-receiver data: 68th Annual Internat. Mtg., Soc. Expl. Geophys., Expanded Abstracts, 1365–1368.

Prucha, M., and Biondi, B., 2002a, Subsalt event regularization with steering filters: 72th Ann. Internat. Meeting, Soc. Expl. Geophysics, Expanded Abstracts, 824–827.

Prucha, M. L., and Biondi, B. L., 2002b, Subsalt event regularization with steering filters: SEP-111, 1–17.

Prucha, M. L., Clapp, R. G., and Biondi, B. L., 1998, Imaging under the edges of salt bodies: Analysis of an Elf North Sea dataset: SEP-97, 35–44.

Prucha, M., Biondi, B., and Symes, W., 1999, Angle-domain common image gathers by wave-equation migration: 69th Ann. Internat. Meeting, Soc. Expl. Geophysics, Expanded Abstracts, 824–827.

Prucha, M. L., Clapp, R. G., and Biondi, B. L., 2001, Imaging under salt edges: A regularized least-squares inversion scheme: SEP-108, 91–104.

- Ronen, S., and Liner, C. L., 2000, Least-squares DMO and migration: *Geophysics*, **65**, no. 5, 1364–1371.
- Stolk, C., and De Hoop, M. V. Seismic inverse scattering in the 'wave-equation' approach: Preprint 2001-047, The Mathematical Sciences Research Institute, 2001. <http://msri.org/publications/preprints/2001.html>.
- Stolk, C., and Symes, W., 2002, Artifacts in Kirchhoff common image gathers: 72nd Annual Internat. Mtg., Soc. Expl. Geophys., Expanded Abstracts, 1129–1132.
- Stolk, C. C., and Symes, W. W., 2004, Kinematic artifacts in prestack depth migration: *Geophysics*, **69**, 562–575.
- Tarantola, A., 1986, A strategy for nonlinear elastic inversion of seismic reflection data: *Geophysics*, **51**, no. 10, 1893–1903.
- ten Kroode, A. P. E., Smit, D.-J., and Verdel, A. R., 1994, Linearized inverse scattering in the presence of caustics: SPIE - Conference on Mathematical Methods in Geophysical Imaging, 1247.
- Tikhonov, A. N., and Arsenin, V. Y., 1977, *Solution of ill-posed problems*: John Wiley and Sons.
- Xu, S., Chauris, H., Lambare, G., and Noble, M., 2001, Common angle image gather - A strategy for imaging complex media: *Geophysics*, **66**, no. 6, 1877–1894.

